Low lateral divergence 2 μm InGaSb/ AlGaAsSb broad-area quantum well lasers

Jiamin Rong,[1,2,4] Enbo Xing,[1,2,4] Yu Zhang,[3] Lijie Wang,[1] Shili Shu,[1] Sicong Tian,[1] Cunzhu Tong,[1,*] Xiaoli Chai,[3] Yingqiang Xu,[3] Haiqiao Ni,[3] Zhichuan Niu,[3] and Lijun Wang[1]

[1]*State Key laboratory of Luminescence and Applications, Changchun Institute of Optics, Fine Mechanics and Physics, Chinese Academy of Sciences, Changchun 130033, China*
[2]*The University of Chinese Academy of Sciences, Beijing 100049, China*
[3]*Institute of Semiconductors, Chinese Academy of Sciences, Beijing 100083, China*
[4]*These authors contributed equally to this work*
[*]*tongcz@ciomp.ac.cn*

Abstract: High power and high brightness mid-infrared GaSb based lasers are desired for many applications, however, the high lateral divergence is still the influence factor for practical application. In this paper, a simple and effective approach based on the fishbone-shape microstructure was proposed, the effective improvement on both the lateral divergence and output power of 2 μm GaSb based broad-area lasers was demonstrated. The lateral divergence is reduced averagely by 55% and 15.8° for 95% power content is realized. The continuous-wave emission power is increased about 19% with the decreased threshold current. The other merits for this microstructure are the unchanged intrinsic characteristic of broad-area lasers and the low cost fabrication.

OCIS codes: (140.5960) Semiconductor lasers; (140.2020) Diode lasers; (140.3070) Infrared and far-infrared lasers; (140.3300) Laser beam shaping.

References and links

1. S. Karsten, L. Samir, K. Philpp, and F. Peter, "2μm laser sources and their possible applications," in *Frontiers in Guided Wave Optics and Optoelectronics*, P. Bishnu, ed. (Intech, 2010).
2. Q. Gaimard, M. Triki, T. Nguyen-Ba, L. Cerutti, G. Boissier, R. Teissier, A. Baranov, Y. Rouillard, and A. Vicet, "Distributed feedback GaSb based laser diodes with buried grating: a new field of single-frequency sources from 2 to 3 μm for gas sensing applications," Opt. Express **23**(15), 19118–19128 (2015).
3. E. Geerlings, M. Rattunde, J. Schmitz, G. Kaufel, H. Zappe, and J. Wagner, "Widely tunable GaSb-based external cavity diode laser emitting around 2.3 μm," IEEE Photonics Technol. Lett. **18**(18), 1913–1915 (2006).
4. G. Belenky, L. Shterengas, J. G. Kim, R. Martinelli, S. Suchalkin, and M. Kisin, "GaSb-based lasers for spectral region 2–4 μm: challenges and limitations," Proc. SPIE **5732**, 169–174 (2005).
5. Y. Rouillard, F. Genty, A. Perona, A. Vicet, D. A. Yarekha, G. Boissier, P. Grech, A. N. Baranov, and C. Alibert, "Edge and vertical surface emitting lasers around 2.0–2.5 μm and their applications," Philos. Trans. A **359**(1780), 581–597 (2001).
6. M. Muller, M. Rattunde, G. Kaufel, J. Schmitz, and J. Wagner, "Short-pulse high-power operation of GaSb-based diode lasers," IEEE Photonics Technol. Lett. **21**(23), 1770–1772 (2009).
7. A. Gassenq, T. Taliercio, L. Cerutti, A. N. Baranov, and E. Tournie, "Mid-IR lasing from highly tensile-strained, type II, GaInAs/GaSb quantum wells," Electron. Lett. **45**(25), 1320–1321 (2009).
8. M. Rattunde, J. Schmitz, G. Kaufel, M. Kelemen, J. Weber, and J. Wagner, "GaSb-based 2.X μm quantum-well diode lasers with low beam divergence and high output power," Appl. Phys. Lett. **88**(8), 081115 (2006).
9. S. Jung, G. Kipshidze, R. Liang, S. Suchalkin, L. Shterengas, and G. Belenky, "Gasb-based mid-infrared single lateral mode lasers fabricated by selective wet etching technique with an etch stop layer," J. Electron. Mater. **41**(5), 899–904 (2012).
10. R. B. Swint, T. S. Yeoh, V. C. Elarde, J. J. Coleman, and M. S. Zediker, "Curved waveguides for spatial mode filters in semiconductor lasers," IEEE Photonics Technol. Lett. **16**(1), 12–14 (2004).
11. H. Wenzel, P. Crump, J. Fricke, P. Ressel, and G. Erbert, "Suppression of higher-order lateral modes in broad-area diode lasers by resonant anti-guiding," IEEE J. Quantum Electron. **49**(12), 1102–1108 (2013).
12. M. T. Cha and R. Gordon, "Spatially filtered feedback for mode control in vertical-cavity surface-emitting lasers," J. Lightwave Technol. **26**(24), 3893–3900 (2008).
13. M. Lichtner, V. Z. Tronciu, and A. G. Vladimirov, "Theoretical investigation of striped and non-striped broad area lasers with off-axis feedback," IEEE J. Quantum Electron. **48**(3), 353–360 (2012).

#258375 Received 29 Jan 2016; revised 24 Feb 2016; accepted 8 Mar 2016; published 25 Mar 2016

14. H. Wenzel, E. Bugge, M. Dallmer, F. Dittmar, J. Fricke, K. H. Hasler, and G. Erbert, "Fundamental-lateral mode stabilized high-power ridge-waveguide lasers with a low beam divergence," IEEE Photonics Technol. Lett. **20**(3), 214–216 (2008).
15. H. K. Choi, J. N. Walpole, G. W. Turner, M. K. Conners, L. J. Missaggia, and M. J. Manfra, "GaInAsSb–AlGaAsSb tapered lasers emitting at 2.05 μm with 0.6 W diffraction-limited power," IEEE Photonics Technol. Lett. **10**(7), 938–940 (1998).
16. P. Crump, P. Leisher, T. Matson, V. Anderson, D. Schulte, J. Bell, J. Farmer, M. DeVito, R. Martinsen, Y. K. Kim, K. D. Choquette, G. Erbert, and G. Tränkle, "Control of optical mode distribution through etched microstructures for improved broad area laser performance," Appl. Phys. Lett. **92**(13), 131113 (2008).
17. S. Forouhar, R. M. Briggs, C. Frez, K. J. Franz, and A. Ksendzov, "High-power laterally coupled distributed-feedback GaSb-based diode lasers at 2 μm wavelength," Appl. Phys. Lett. **100**(3), 031107 (2012).
18. M. T. Kelemen, J. Weber, M. Mikulla, and G. Weimann, "High-power high-brightness tapered diode lasers and amplifiers," Proc. SPIE **5723**, 198–208 (2005).
19. J. Hecht, "Bringing high brightness to high-power laser diodes," Laser Focus World **47**(11), 43–46 (2011).
20. V. P. Kalosha, K. Posilovic, and D. Bimberg, "Lateral-Longitudinal modes of high-power inhomogeneous waveguide lasers," IEEE J. Quantum Electron. **48**(2), 123–128 (2012).
21. P. Crump, S. Boldicke, C. M. Schultz, H. Ekhteraei, H. Wenzel, and G. Erbert, "Experimental and theoretical analysis of the dominant lateral waveguiding mechanism in 975 nm high power broad area diode lasers," Semicond. Sci. Technol. **27**(4), 045001 (2012).
22. A. F. Jonathan, A. B. Mikhail, and C. Federico, "Wide-ridge metal-metal terahertz quantum cascade lasers with high-order lateral mode suppression," Appl. Phys. Lett. **92**(3), 031106 (2008).
23. P. Crump, M. Ekterai, C. M. Schultz, G. Erbert, and G. Tränkle, "Studies of limitations to lateral brightness in high power diode lasers using spectrally-resolved mode profiles," in *Proceedings of IEEE International Semiconductor Laser Conference* (IEEE, 2014), pp. 23–24.

1. Introduction

High power and high brightness mid-infrared GaSb based lasers are very attractive for gas sensing, liquid sensing, light detection and ranging (LiDAR), laser spectroscopy and medical applications [1–5], and the lasers based on broad-area (BA) structure have been widely studied [6–8] because BA structure is beneficial for high power emission. However, the penalty for BA lasers (BALs) is the deteriorative beam quality due to the allowance of multi-mode operation resulted by the wide waveguide. Moreover, the emission properties in BALs are determined by the complex interplay between the laterally extended waveguide, and the nonlinear, local interaction of the intense light field with the semiconductor active medium, in which the filamentation is caused because of the strongly coupling of gain and refractive index. Hence the controlling of lateral modes in BALs is crucial for the realization of high power and high brightness. Some approaches to control the lateral modes and suppress filamentation in mid-infrared and near-infrared lasers have been proposed, for instance, selective wet etching [9], curved waveguide [10], anti-guiding layer [11], the use of external cavities [12,13], leaky ridge-waveguide [14], tapered gain regions [15], etched microstructures [16] and Bragg gratings [17]. Although the tapered gain regions have achieved the diffraction limited beam quality [15,18], the long and narrow ridge section used as mode filtering limits the total cavity length, the volume of gain medium, thermal dissipation area and hence the possible highest power [18]. So generally tapered laser has more than twice as high as for the BAL on the threshold current density and thermal dissipation energy density [18]. Another disadvantage for tapered laser is the astigmatism, which makes optics design for modules more complex and packaging more challenging [19]. Therefore, a simple, effective approach without largely shrinking the volume of gain material is desired for the improvement of lateral beam quality of BALs.

In this paper, we proposed a symmetric microstructure to suppress the high order lateral modes of GaSb based BALs. The lasing spectra, light-injected current-voltage (L-I-V) characteristics and lateral far-field (FF) performance were measured and analyzed. The simulation and experimental results demonstrated that this microstructure was able to effectively reduce the number of lateral modes, improve the lateral divergence and output power. The organization of this paper is as follows, section 2 shows the simulation results by finite-difference time-domain (FDTD) software, and section 3 is about the device fabrication. The discussing and analyzing of experimental results are shown in section 4. The conclusions are summarized in section 5.

#258375 Received 29 Jan 2016; revised 24 Feb 2016; accepted 8 Mar 2016; published 25 Mar 2016

2. Simulation

For the BA structure, the major energy of fundamental mode localizes at the center of stripe [20,21], so two rows of symmetrical trenches with linearly increasing lengths are proposed to suppress the high order lateral modes. The detailed structure is shown in Fig. 1(a). The length of trenches [*L* in Fig. 2(b)] in microstructure increases from 5 μm to 35 μm by 5 μm step, the width of single trench is 4 μm with a period of 9 μm and the total width [*W* in Fig. 2(b)] is 76 μm. The trench is formed by etching, which means the inside is air. Two-dimensional FDTD simulation is performed and the results are respectively shown in Figs. 1(b)-1(f) for fundamental mode, mode 2, 3, 5 and 10, which reveal the modal field distribution $E(x,y)$ in waveguide after passing the microstructure. In this simulation, the effective index is 3.512, which is calculated by the Lumerical Mode Solutions software. The stripe width is 100 μm (along the longitudinal coordinate *y*). The lateral coordinate *x* represents the distance from the front facet. As can be seen, there exists obvious field intensity localized in the trenches for the high order lateral modes, which means that the microstructure provides extra loss in the lateral direction, and the higher order mode suffers higher loss. It is worth noting that seven trenches have localized the adequate energy of mode-2, mode-3 and mode-5 in the trenches. Considering more trenches will cause more losses for fundamental mode, seven trenches are chosen in the realistic experiment.

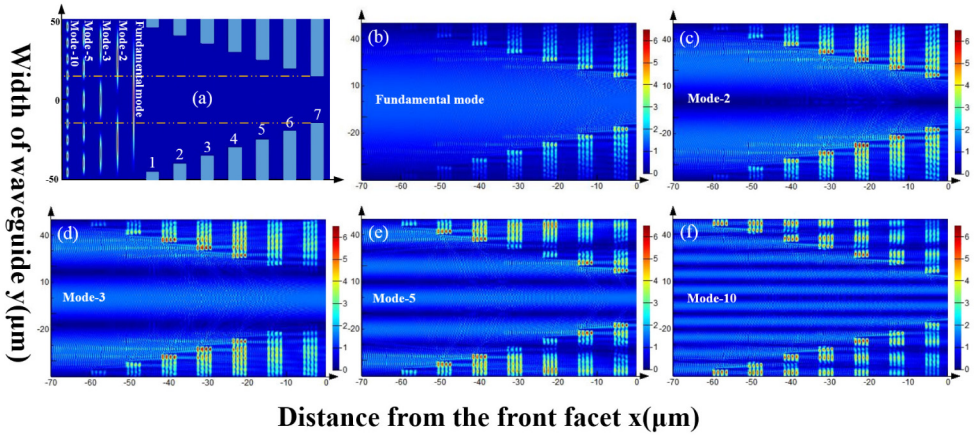

Fig. 1. (a) Detail on the fishbone microstructure in the realistic device, (b)-(f) are the calculated optical field distribution after the different mode transmitting through the microstructure with stripe width of 100 μm (see also Visualization 1).

3. Device fabrication

GaSb based laser structure was grown on (100)-oriented 2-inch GaSb substrate by a solid-source VEECO Gen II molecular beam epitaxy (MBE) system. The active region of laser shown in Fig. 2 consists of two 10 nm $In_{0.18}Ga_{0.82}Sb$ quantum wells (QWs) separated by 20 nm lattice matched $Al_{0.35}Ga_{0.65}As_{0.02}Sb_{0.98}$ barrier layer. The active region was sandwiched between the symmetrical top and bottom 250 nm thick $Al_{0.35}Ga_{0.65}As_{0.02}Sb_{0.98}$ waveguide layers. The top and bottom were respectively 2 μm thick $Al_{0.60}Ga_{0.40}As_{0.02}Sb_{0.98}$ p-doped and n-doped cladding layers. As to n-type and p-type dopants, tellurium and beryllium were used respectively. For low resistance contact, a 250 nm thick p + GaSb layer was grown on the top of cladding layer. The total thickness of the epitaxy layers was about 6 μm.

#258375 Received 29 Jan 2016; revised 24 Feb 2016; accepted 8 Mar 2016; published 25 Mar 2016

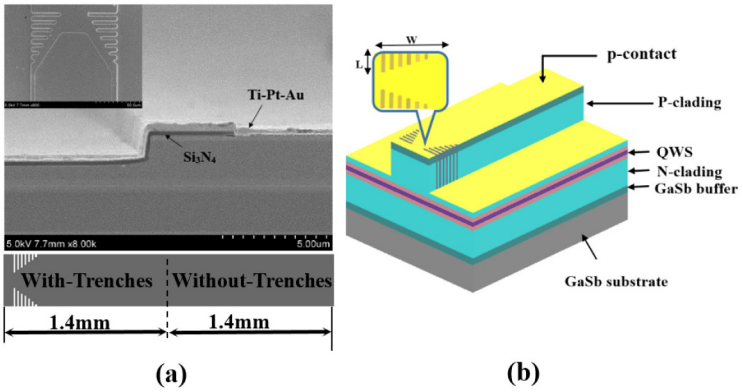

Fig. 2. (a) Scanning electron microscope photographs of GaSb based BAL with the fishbone microstructure, (b) schematic diagram of device structure.

After the MBE growth, the standard processing techniques of semiconductor lasers were used for fabrication. It is worthy to note that the processing is totally same as the conventional BALs, the only difference is the mask pattern for stripe definition. This means that he approach used in this paper will not increase the fabrication cost, which is very meaningful for low-lost and high-volume production. The stripe mesa with the width of 100 μm was fabricated using standard optical lithography. The trenches were defined by ICP etching with depth of 1.6 μm, followed by PECVD deposition of 200 nm Si_3N_4 at 300 °C as electrical insulation layer. The contact window opening was performed by reactive ion etching of the SiN_x insulation layer using SF_6/O_2 gas. Then the p-type contact metal of Ti-Pt-Au was deposited and the unwanted metal on the microstructure was removed using standard lift-off techniques. After the backside thinning and polishing, Au-Ge-Ni-Au contact layer was grown on the backside of wafer. For the purpose of accurate comparison, the devices with (WT) and without (W/O) fishbone microstructure were fabricated with the same cavity length of 1.4 mm by cleaving from a same stripe just as shown in Fig. 2(a). Finally the BALs were soldered on the copper heat-sink using indium by p-side down without facet passivation and coating for testing. The FF patterns and profiles were measured by the laser beam profiler with type of Pyrocam III, the lasing spectrum was measured by Bruker Vertex 70 FTIR spectrometer.

4. Results and discussion

4.1 L-I-V characteristics

The measured L-I-V curves for InGaSb/AlGaAsSb QW BALs with and without microstructure at room temperature are shown in Fig. 3. The devices operate under continuous wave (CW) mode. It can be seen that the voltage performances for WT and W/O devices are almost the same, but the WT device shows an evident improvement in the output power. The maximum powers (both facets) are respectively 338 mW for WT device and 285 mW for W/O device. In the other word, about 19% increase in the output power is realized by the fishbone microstructure. Moreover, the threshold current and slope efficiency are also improved. The slope efficiency for WT device is increased to 0.225 W/A, by contrast it is ~0.19 W/A for the W/O device. The maximum output powers of these samples are limited by the thermal rollover according to Fig. 3. The increased output power might be due to the suppressing of high order lateral modes [16,22], which reduce the mode competition and lead to a more uniform near field and better matching between the mode profile and injected current profile [16]. Although the enhanced heat dissipation from the deeply etched trenches seems like also one of the reasons, the influence is small because the area of trenches is just 0.8% of the whole contact area. A heat simulation using ANSYS software reveals the improvement of temperature at active region due to the microstructure is only 0.3 °C.

#258375 Received 29 Jan 2016; revised 24 Feb 2016; accepted 8 Mar 2016; published 25 Mar 2016

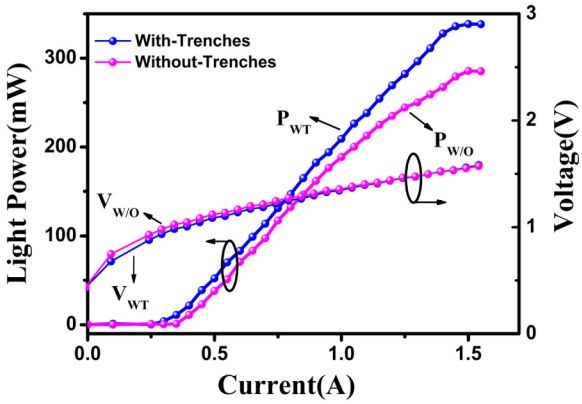

Fig. 3. L-I-V characteristics of InGaSb/AlGaAsSb QW BALs with and without microstructure at room temperature.

4.2 Spectrum property

Figure 4 shows the measured lasing spectra of these two kinds of laser devices at injection current of 0.8 A and 1.5 A. Obviously the microstructure reduces significantly the mode number. As shown in Fig. 4(a), the spectrum span for the W/O device at 0.8 A is up to 25 nm and the emitting peaks are over ten. However, the peak number goes down to about three for the devices with microstructure, and it is only five when the current is increased to 1.5 A, which is still far less than that of W/O devices. The main wavelength is about 1996.7 nm at 0.8 A for device with microstructure, this value shifts to 2027.1 nm at 1.5 A. More detailed analysis on the modes is difficult because of the lacking of the spectrally-resolved near field and FF profiles [23], however, the ability of mode controlling for this fishbone microstructure is confirmed.

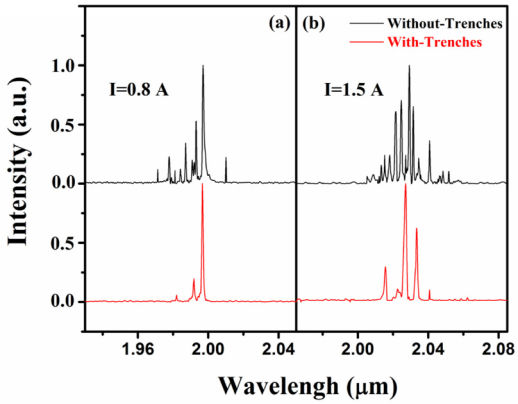

Fig. 4. Measured emission spectra of GaSb based BALs without and with microstructure at 0.8 A (a) and 1.5 A (b).

4.3 Far-field characteristics

To further verify the advantage of the introduced microstructure on the BALs, the vertical and lateral FF characteristics are measured and shown in Fig. 5 and Fig. 6, respectively. Because the microstructure is designed according to the lateral mode distribution and only plays the role in lateral divergence, it should not affect the FF in vertical direction, which is confirmed by Fig. 5. The corresponding vertical FF angle is about 61.1° for full-width at half-maximum

#258375 Received 29 Jan 2016; revised 24 Feb 2016; accepted 8 Mar 2016; published 25 Mar 2016

(FWHM) definition and almost same for W/O and WT devices. Figures 6(a)-6(c) show that the

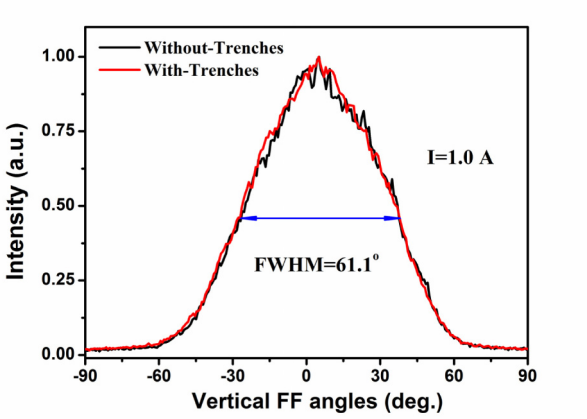

Fig. 5. Vertical FF profiles of GaSb based BALs at 1.0 A.

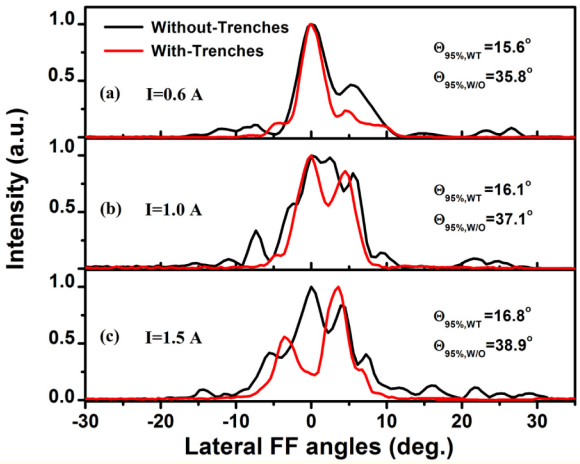

Fig. 6. Lateral FF angles of GaSb based BA lasers at 0.6 A (a), 1.0 A (b) and 1.5 A (c).

lateral FF profiles at 0.6 A, 1.0 A and 1.5 A, respectively. It can be seen that the microstructure is able to reduce evidently the side-lobes in the lateral FF and hence improve the lateral divergence. Note that the FWHM definition of FF angle is not able to reflect the intrinsic characteristics of lateral FF here due to the existence of so many side-lobes, FF angles defined with 95% power content are applied. An improvement of 56.4% is realized at 0.6 A using the fabricated microstructure. When the injected current increases from 0.6 A to 1.5 A, the lateral FF angles gradually increase from 15.6° to 16.8° ($\Theta_{95\%, WT}$) for WT devices. The corresponding values vary from 35.8° to 38.9° ($\Theta_{95\%, W/O}$) for the W/O devices. The improvement is 56.8% at 1.5 A. To avoid the testing error, the experimental data of three group devices are obtained and listed in Table 1. It shows that the averaged improvement in the lateral FF angle is about 55.0%. Considering the beam quality of mid-infrared GaSb based BALs in the lateral direction is generally very poor, more than 50% improvement is extremely meaningful.

#258375 Received 29 Jan 2016; revised 24 Feb 2016; accepted 8 Mar 2016; published 25 Mar 2016

Table 1. Measured Performance of GaSb Based QW BALs at 1.5 A for Three Group Devices

Groups		Voltage (V)	Power (mw)	Lateral angles (deg., 95% power content)	Improvement of lateral FF angles
Group 1	WT	1.536	338	16.8	56.8%
	W/O	1.543	285	38.9	
Group 2	WT	1.530	301	17.2	55.3%
	W/O	1.532	283	38.5	
Group 3	WT	1.539	339	18.7	53.0%
	W/O	1.548	293	39.8	

5. Conclusion

In conclusion, we had demonstrated the improved lateral divergence in 2 μm GaSb based QW BALs using a simple fishbone-shape microstructure designed according to the distribution of lateral modes. It was shown that the proposed microstructure could effectively reduce the mode number, and an average improvement of 55% in lateral divergence with 95% power content was realized. The other benefits from this microstructure were the improved threshold current and output power. Although the decreased divergence is not as perfect as diffraction limitation, the potential possibility for high power, high beam quality operation and the compatibility for low cost fabrication are the merits. We believe these results will contribute to the development of high power and low divergence mid-infrared GaSb based diode lasers.

Acknowledgments

This work was supported by National Natural Science Foundation of China (NSFC) (No. 61404138, and 61435012), the International Science Technology Cooperation Program of China (No. 2013DFR00730), National Basic Research Program of China (2013CB643903) and Science and Technology Development Projects of Jilin Province (20150520105JH).

#258375 Received 29 Jan 2016; revised 24 Feb 2016; accepted 8 Mar 2016; published 25 Mar 2016